Available online at www.sciencedirect.com
SCIENCE DIRECT®
Journal of Sound and Vibration 279 (2005) 739–756
JOURNAL OF SOUND AND VIBRATION
www.elsevier.com/locate/jsvi

Minimizing vibration response of cylindrical shells through layout optimization of passive constrained layer damping treatments

H. Zheng[a,*], C. Cai[a], G.S.H. Pau[b], G.R. Liu[b]

[a] *Institute of High Performance Computing, 1 Science Park Road, #01-01 The Capricorn, Singapore Science Park II, Singapore 117528, Singapore*

[b] *Singapore-MIT Alliance, The National University of Singapore, 10 Kent Ridge Crescent, Singapore 119260, Singapore*

Received 7 January 2003; accepted 14 November 2003

Abstract

A layout optimization of passive constrained layer damping (PCLD) treatment for minimizing the vibration response of cylindrical shells is presented with consideration of broadband transverse force excitation. The equations governing the displacement responses, relating the integrated out-of-plane displacement over the whole structural volume, i.e., the structural volume displacement (SVD), of a cylindrical shell to structural parameters of base structure and multiple PCLD patches, are derived using the energy approach and assumed-mode method. Genetic algorithm (GA) based penalty function method is employed to find the optimal layout of rectangular PCLD patches with aim to minimize the SVD of the PCLD-treated cylindrical shell. Optimization solutions of the locations of patches for PCLD treatment are obtained under the constraint of total amount of PCLD materials in terms of percentage added weight to the base structure. Effects due to number of patches, their aspect ratios, and total amount of added PCLD weight are also studied. Examination of the optimal layouts reveals that the patches tend to increase their coverage in the axial direction and distribute over the whole surface of the cylindrical shell for optimal SVD reduction.
© 2003 Elsevier Ltd. All rights reserved.

1. Introduction

Passive constrained layer damping (PCLD) treatment has been an effective way to suppress vibrations of and sound radiation from various structures. The pioneer work in the field could be

*Corresponding author.
E-mail address: zhengh@ihpc.a-star.edu.sg (H. Zheng).

0022-460X/$ - see front matter © 2003 Elsevier Ltd. All rights reserved.
doi:10.1016/j.jsv.2003.11.020

traced back to late 1950s when Kerwin [1] derived an expression for an effective, complex, flexural stiffness of the three-layer beams with damping core layer. His work was followed by a number of investigations. DiTaranto [2] and Mead and Markus [3] extended Kerwin's work and developed a sixth order equation of motion governing the transverse displacement of a sandwich beam with arbitrary boundary conditions. After that, different formulations and techniques have been reported, e.g., Refs. [4–6]. The problem of computing damped natural frequencies and loss factors is explicitly solved [7,8] for both beams and plates when simply support end conditions are assumed. Analytical–numerical procedures are proposed to solve the problem when different boundary conditions are assumed [9].

Most of these early works dealt with full coverage PCLD treatments that are evidently not practical in purpose. For partially covered viscoelastically damped sandwich beams or plates, Nokes and Nelson [10] were among the earliest investigators to provide the solution to the problem. A more thorough analytical study was carried out by Lall et al. who solved, by using three different approaches, the eigenvalue problem for a beam [11] and for a plate [12] with a single damping patch. Kung and Singh [13] presented a refined method for analyzing the modal damping of beams with multiple constrained-layer viscoelastic patches.

In addition to all above-described works on passive constrained layer damping (PCLD) treatments for vibration suppression of beams and plates, the study of vibration and damping in shells with added damping treatment has also been of interest to many researchers. Pan [14] studied the axisymmetrical vibration of a finite length cylindrical shell with a viscoelastic core. Jones and Salerno [15] investigated the effect of damping on the forced axisymmetrical vibration of cylindrical shells with a viscoelastic core. Alam and Asnani [16,17] carried out the vibration and damping analysis of a general multilayered cylindrical shell consisting of an arbitrary number of elastic and viscoelastic layers with simply supported end conditions. Ramesh and Ganesan [18] used a finite element method to solve for a cylinder-absorber system with thin axial strips which bonded to the cylinder with a thin viscoelastic layer. Hu and Huang [19] developed a generic theory for the PCLD treated shell with full coverage. Recently, Chen and Huang investigated the damping effects of PCLD treatment of strip type along longitudinal direction [20] and along circumference [21], respectively, on the forced response of a cylindrical shell. A thin shell theory in conjunction with the Donnell–Mushtari–Vlasov assumptions is employed to yield their mathematical model. Their parametric studies showed that thicker or stiffer CL warrants better damping, and thicker VEM does not always give better damping than thinner ones when CL exceeds a certain thickness.

These theoretical works and parametric studies on PCLD treatments for vibration and noise suppression really provide assistance to design decision. However, studies based on the optimization are quite less, particularly, in the optimum design of partial PCLD treatment of cylindrical shell, there has been no existing literature to the authors' knowledge. Marcelin et al. [22] considered the partially covered beam structure and optimization with design variables being the dimensions and the locations of all the viscoelastic layers. Special beam finite elements were used to represent the behavior of the sandwich parts of the beam. Both theory and experiment [23] show that for stiff viscoelastic layers the loss factor is greater for partial coverage than for full coverage. Chen and Huang [24] presented a study on optimal placement of PCLD treatment for vibration suppression of plates. In their optimization, the structural damping plays the main performance index and the frequencies' shift and PCLD thickness play as penalty functions.

Topographical and complex optimal solution techniques were employed in searching for the optimal value of CLD treatment.

The study presented in this paper attempts to arrive at an optimum design of partial PCLD treatment of cylindrical shell by finding an optimal layout of multiple rectangular PCLD patches of fixed thickness and material properties to minimize the forced vibration response under a broadband transverse excitation. The equations relating the integrated out-of-plane displacement over the whole structural volume, i.e., the structural volume displacement (SVD), of a cylindrical shell to structural parameters of base structure and multiple PCLD patches are derived using energy based approach and assumed-mode method. Genetic algorithm (GA) based penalty function method is employed to find the optimal layout of rectangular PCLD patches with aim to minimize the SVD of PCLD-treated cylindrical shell. Optimization solutions of rectangular PCLD patches' locations and dimensions are obtained under the constraint of total amount of PCLD in terms of percentage added weight to the base structure. Effects due to the number of patches and their aspect ratios, and total amount of added PCLD weight are also studied, towards maximum vibration attenuation using minimum amount of PCLD patches.

2. Analytical model and formulation

2.1. Kinematic relation

A cylinder treated with multiple PCLD patches is modelled as a composite cylindrical shell consisting of three layers, namely the base, constraining and viscoelastic layers, each referred to by using the subscripts/superscripts s, c and v, respectively. A general configuration for a simply supported cylinder treated with a PCLD patch p is shown in Fig. 1, with labeled design parameters and design variables. With consideration of simplicity in patch fabrication, the thickness and material property of constraining layer and viscoelastic core, respectively, are assumed same for all patches. The layers have different thickness denoted by h_i, where $i = s$, c or

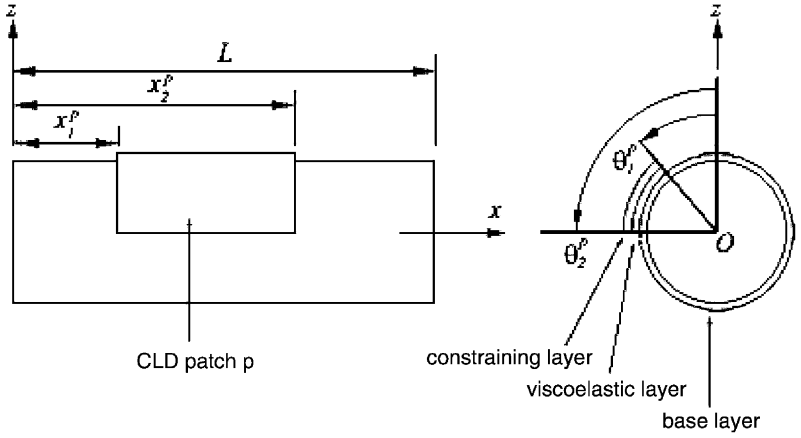

Fig. 1. A simply-supported cylinder with one partial PCLD patch.

v. Then, the mathematical model for the cylinder is derived following the procedure given by Chen and Huang [20,21], but not limited to PCLD treatment of strip type along longitudinal direction and along circumference.

Under the Donnell–Mushtari–Vlasov assumptions [25], the stress–strain relationship in cylindrical shell and in constraining layer are described by

$$\sigma_{xx}^{i} = \frac{E_i}{1-\upsilon_i^2}(\varepsilon_{xx}^{i} + \upsilon_i \varepsilon_{\theta\theta}^{i}),$$

$$\sigma_{\theta\theta}^{i} = \frac{E_i}{1-\upsilon_i^2}(\varepsilon_{\theta\theta}^{i} + \upsilon_i \varepsilon_{xx}^{i}), \quad i = s, c,$$

$$\sigma_{x\theta}^{i} = G_i \varepsilon_{x\theta}^{i}, \tag{1}$$

where E_i, G_i, v_i denote Young's modulus, shear modulus, and the Poisson ratio, respectively, of the material, σ the stress and ε the strain in the layers.

As the cylinder is approximated by a thin shell, the displacements in x and θ directions are assumed, as in Ref. [20], to vary linearly through the shell thickness, and the displacement in the transverse direction is independent of z. Thus, the strain-displacement relations is given by

$$\varepsilon_{xx}^{i} = \frac{\partial u_x^i}{\partial x} - z\frac{\partial^2 u_x^i}{\partial x^2},$$

$$\varepsilon_{\theta\theta}^{i} = \frac{1}{r_i}\frac{\partial u_\theta^i}{\partial \theta} + \frac{u_z^i}{r_i} - \frac{z}{r_i^2}\frac{\partial^2 u_z^i}{\partial \theta^2}, \quad i = s, c,$$

$$\varepsilon_{x\theta}^{i} = \frac{\partial u_\theta^i}{\partial x} + \frac{1}{r_i}\frac{\partial u_x^i}{\partial \theta} - 2\frac{z}{r_i^2}\frac{\partial^2 u_z^i}{\partial x \partial \theta}, \tag{2}$$

where r_i $(i = s, c)$ represent the radius of the base cylinder and constraining, respectively; u_x, u_θ, and u_z denote the displacements in axial, circumferential, and radial directions. For the viscoelastic layer, the stress relation is given by

$$\sigma_{xz}^{v} = G_v^* \varepsilon_{xz}^{v},$$

$$\sigma_{\theta z}^{v} = G_v^* \varepsilon_{\theta z}^{v}, \tag{3}$$

where G_v^* is the complex shear modulus of the viscoelastic material, $G_v^* = G_v(1 + j\eta_v)$ with η_v the damping loss factor. The strain–displacement relation of the viscoelastic layer is given by

$$\varepsilon_{xz}^{v} = \beta_x^v + \frac{\partial u_z^v}{\partial x},$$

$$\varepsilon_{\theta z}^{v} = \beta_\theta^v - \frac{u_\theta^v}{r_v} + \frac{1}{r_v}\frac{\partial u_z^v}{\partial \theta}, \tag{4}$$

where β_x^v and β_θ^v are the angular displacements of the viscoelastic layer, respectively, in axial and tangential directions, and r_v is its radius. Taking into consideration the Love simplifications, the

assumption of no-slip condition between layers and $u_z^i = u_z$, where $i = s, c, v$, yields

$$\varepsilon_{xz}^v = \frac{1}{h}(u_x^c - u_x^s) + \frac{1}{2h_v}(h_c + h_z + 2h_v)\frac{\partial u_z}{\partial x},$$
$$\varepsilon_{\theta z}^v = \left(\frac{1}{h_v} - \frac{1}{2r_v}\right)u_\theta^c - \left(\frac{1}{h_v} + \frac{1}{2r_v}\right)u_\theta^s + \left(\frac{h_c}{2h_v r_c} + \frac{h_s}{2h_v r_s} - \frac{h_c}{4r_v r_c} + \frac{h_s}{4h_v r_s} + \frac{1}{r_v}\right)\frac{\partial u_z}{\partial \theta}. \tag{5}$$

2.2. Energy expressions

The kinetic energies of the layers with neglected in-plane inertia are

$$T_s = \tfrac{1}{2} r_s \rho_s h_s \int_0^L \int_0^{2\pi} \dot{u}_z^2 \, \mathrm{d}x,$$
$$T_v = \tfrac{1}{2} r_v \rho_v h_v \sum_{p=1}^{n_p} \int_{x_1^p}^{x_2^p} \int_{\theta_1^p}^{\theta_2^p} \dot{u}_z^2 \, \mathrm{d}x,$$
$$T_c = \tfrac{1}{2} r_c \rho_c h_c \sum_{p=1}^{n_p} \int_{x_1^p}^{x_2^p} \int_{\theta_1^p}^{\theta_2^p} \dot{u}_z^2 \, \mathrm{d}x. \tag{6}$$

Here the dot indicates derivative with respect to time; and $p = 1, 2, \ldots, n_p$ with n_p the number of PCLD patches. The strain energies are

$$U_s = \frac{r_s}{2} \int_{-h_s/2}^{h_s/2} \int_0^L \int_0^{2\pi} \left[\frac{E_s}{1-\upsilon_s^2}(\varepsilon_{xx}^{s^2} + \varepsilon_{\theta\theta}^{s^2}) + \frac{2E_s\upsilon_s}{1-\upsilon_s^2}(\varepsilon_{xx}^s \varepsilon_{\theta\theta}^s) + G_s \varepsilon_{x\theta}^{s^2}\right] \mathrm{d}\theta \, \mathrm{d}x \, \mathrm{d}z,$$
$$U_v = \frac{r_v}{2} \sum_{p=1}^{n_p} \int_{-h_v/2}^{h_v/2} \int_{x_1^p}^{x_2^p} \int_{\theta_1^p}^{\theta_2^p} (G_v \varepsilon_{xz}^{v^2} + G_v \varepsilon_{\theta z}^{v^2}) \, \mathrm{d}\theta \, \mathrm{d}x \, \mathrm{d}z,$$
$$U_c = \frac{r_c}{2} \sum_{p=1}^{n_p} \int_{-h_c/2}^{h_c/2} \int_{x_1^p}^{x_2^p} \int_{\theta_1^p}^{\theta_2^p} \left[\frac{E_c}{1-\upsilon_c^2}(\varepsilon_{xx}^{c^2} + \varepsilon_{\theta\theta}^{c^2}) + \frac{2E_c\upsilon_c}{1-\upsilon_c^2}(\varepsilon_{xx}^c \varepsilon_{\theta\theta}^c) + G_c \varepsilon_{x\theta}^{c^2}\right] \mathrm{d}\theta \, \mathrm{d}x \, \mathrm{d}z. \tag{7}$$

Assuming an external load, $f(x, \theta, t)$, a transverse force applied on the cylinder surface, the work done by this force can be expressed as

$$P = \int_0^L \int_0^{2\pi} r_s f(x, \theta, t) w(x, \theta, t) \, \mathrm{d}\theta \, \mathrm{d}x. \tag{8}$$

2.3. Equation of motion

The dynamic response of the PCLD treated cylinder excited by the external transverse load can be calculated by substituting the kinetic and strain energies into Lagrange's equation

$$\frac{\mathrm{d}}{\mathrm{d}t}\left(\frac{\partial T}{\partial \dot{q}_i}\right) - \frac{\partial T}{\partial q_i} + \frac{\partial U}{\partial q_i} = \frac{\partial P}{\partial q_i}, \tag{9}$$

where q_i represents the ith generalized co-ordinate, T and U are, respectively, the kinetic and strain energy of the whole system expressed by

$$T = T_s + T_v + T_c,$$

$$U = U_s + U_v + U_c. \tag{10}$$

For a cylinder, the displacements can be approximated by

$$w(x,\theta,t) = \sum_m \sum_n W_{mn}(x,\theta)\zeta_{mn}(t) = W^{\mathrm{T}}\zeta,$$

$$u_x^s(x,\theta,t) = \sum_m \sum_n U_{mn}^s(x,\theta)\eta_{imn}^s(t) = U^{s^{\mathrm{T}}}\eta^s,$$

$$u_\theta^s(x,\theta,t) = \sum_m \sum_n V_{mn}^s(x,\theta)\xi_{mn}^s(t) = V^{s^{\mathrm{T}}}\xi^s,$$

$$u_x^c(x,\theta,t) = \sum_m \sum_m U_{mn}^c(x,\theta)\eta_{mn}^c(t) = U^{c^{\mathrm{T}}}\eta^c,$$

$$u_\theta^c(x,\theta,t) = \sum_m \sum_n V_{mn}^c(x,\theta)\xi_{mn}^c(t) = V^{c^{\mathrm{T}}}\xi^c, \tag{11}$$

where W, U^i and V^i $(i = s, c)$ are the assumed displacement shapes and ζ, η^i and ξ^i are the generalized co-ordinates of the displacement response in cylinder radial, axial and circumferential directions, respectively.

2.4. Solutions of displacement response

Limiting the problem to the cylinder with simply supported ends, the mode shape functions can be assumed as follows:

$$\begin{aligned} W_{mn}(x,\theta) &= \sin\left(\frac{m\pi x}{L}\right)\cos n(\theta-\phi),\\ U_{mn}^i(x,\theta) &= \cos\left(\frac{m\pi x}{L}\right)\cos n(\theta-\phi), \quad i = s, c,\\ V_{mn}^i(x,\theta) &= \sin\left(\frac{m\pi x}{L}\right)\sin n(\theta-\phi). \end{aligned} \tag{12}$$

Using above shape functions and substituting Eqs. (6)–(8) into Lagrange's Eq. (9) yield the equation of motion of the cylinder in the form

$$[M]\{\ddot{q}\} + [K]\{q\} = \{F\}, \tag{13}$$

where $[M] = [M^s + M^v + M^c]$, the mass matrix, and $[K] = [K^s + K^v + K^c]$, the stiffness matrix of the PCLD-treated cylinder. Vector $\{q\} = [q_\zeta^{\mathrm{T}}, q_\eta^{s^{\mathrm{T}}}, q_\xi^{s^{\mathrm{T}}}, q_\eta^{c^{\mathrm{T}}}, q_\xi^{c^{\mathrm{T}}}]^{\mathrm{T}}$ is a column vector containing the

modal coefficients and $\{F\}$ is the vector of generalized force, of which the first $m \times n$ elements can be written as

$$\{F\}_{m\times n} = \left[-\int_0^L \int_0^{2\pi} r_s f(x,\theta,t) W_{ij}(x,\theta)\,\mathrm{d}\theta\,\mathrm{d}x\right]^{\mathrm{T}},$$
$$i = 1,2,\ldots,m;\ \ j = 1,2,\ldots,n. \tag{14}$$

All others are zeros since only a transverse load is applied on the cylinder surface. Further, considering the case of unit time-harmonic point force with a circular frequency ω, the vector of generalized co-ordinates become

$$\{q\} = \{\tilde{q}\}\mathrm{e}^{\mathrm{j}\omega t} \tag{15}$$

and the generalized transverse load for the (i,j)th modal is

$$F_{ij}(x,\theta,t) = -r_s W_{ij}(x^*,\theta^*)\mathrm{e}^{\mathrm{j}\omega t} = \tilde{F}_{ij}(x^*,\theta^*)\mathrm{e}^{\mathrm{j}\omega t}, \tag{16}$$

where (x^*,θ^*) denotes the location of the transverse load. Under the excitation of this time-harmonic force, the system equation can be written as

$$[-\omega^2 M + K]\{\tilde{q}\} = \{\tilde{F}\}. \tag{17}$$

Solving this system equation yields the solution of generalized displacement at the circular frequency, ω. Multiplying them by the assumed modes for the structure yields the physical displacement response at any location, (x,θ), of the cylinder.

3. PCLD layout optimization

3.1. Objective function

With the objective of minimizing the vibration response of the cylinder, the out-of-plane displacement complex amplitude is obviously the quantity of interest. Since the displacement is location dependent, another quantity representing the global displacement response, i.e., SVD, which is defined as the integration of the displacement over the cylinder surface as

$$D(\omega) = \int_0^L \int_0^{2\pi} |u_z(x,\theta,\omega)| r_s\,\mathrm{d}\theta\,\mathrm{d}x, \tag{18}$$

where $|u_z(x,\theta,\omega)|$ is the module magnitude of complex out-of-plane displacement at cylinder surface location (x,θ). This SVD is a function of the layout of the PCLD patches and the total amount of PCLD material used as well as the excitation level and location. Undoubtedly, minimizing the SVD would lead to significant reductions in the vibrational energy of whole cylinder.

Furthermore, as the SVD depends upon the frequency, an integral criterion over an appropriate frequency range is required for the case of broadband excitation. A solution that meets technical interest is

$$f = \frac{1}{\omega_{\max} - \omega_{\min}} \int_{\omega_{\min}}^{\omega_{\max}} D(\omega)\,\mathrm{d}\omega. \tag{19}$$

Here $\omega_{\min}$ and $\omega_{\max}$ are, respectively, the minimum and maximum excitation frequencies in rad/s. In the optimization that follows, the broadband SVD of the cylinder defined by expression (19) together with Eq. (18) is chosen as the objective function to be minimized.

Note that the SVD originates from active structural acoustic control (ASAC) [26] where, in order to implement the structural sensing strategy, the radiated sound power by a vibrating planar structure is simply related to its SVD in the low frequency region. So minimizing the SVD would lead to significant reductions of the sound power. This terminology is used here just for defining the global displacement response of the cylinder. In ASAC, the SVD is defined as the integration of complex out-of-plane displacement, $u_z(x,\theta,\omega)$, over the whole structure surface. But for the problem here, the SVD is defined as the integration of the module magnitude of displacement, $|u_z(x,\theta,\omega)|$, over the structural surface. Under this definition, certainly, the larger the displacement at any particular point is, the SVD of considered structure would be larger.

3.2. Variables and constraints

Assuming that only rectangular patches are used, the layout of one PCLD patch can be completely defined by four design variables, namely the axial location, angular location, axial length and angular length, as shown in Fig. 2. For the convenience of fabrication, all the PCLD patches are kept same thickness and Young's modulus for constraining layer and viscoelastic layer, respectively. In this circumstance, the number of variables of optimization for the problem, i.e., the design parameters to be optimized, are $4 \times n_p$ provided that n_p patches are used for the treatment.

In real-life vibration control design, the added weight to the base structure owing to CLD treatment is always restricted to a small amount of percentage of the structure. Thus, in the layout optimization, the total amount of PCLD material is fixed in each computation run. The problem is then constrained to ensure physical feasibility in which the patches are bounded within the area of the cylinder surface and do not overlap each other.

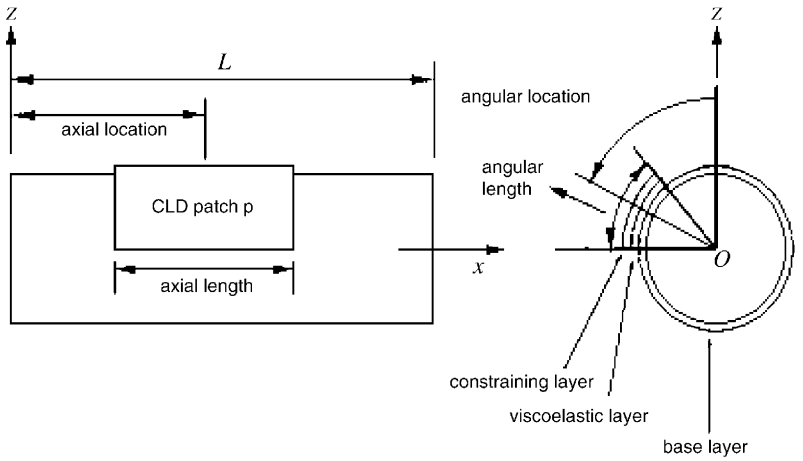

Fig. 2. The four variables to be optimized: axial location, angular location, axial length and angular length.

3.3. Optimization strategy

Several optimization algorithms/methods are available to solve the problem defined by expressions (17)–(19). Most algorithms are designed so far to find a local optimum. One example is the sequential quadratic programming, SQP, algorithm which has shown to be robust and efficient for most optimization problems [27]. However, many optimization problems have several local optima and it is often of interest to find the best optimum in the whole feasible design domain, i.e., the global optimum. Since no mathematical conditions for global optimality exist, a global optimum is usually more difficult and time consuming to find than a local optimum. Some methods have, nevertheless, been developed to find an approximation of the global optimum without scanning the whole feasible design domain. The genetic algorithm, or shortly GA, is such a method that is developed to search for the approximation of global optimum. The GA has been used previously by a lot of researchers to solve various non-linear optimization problems [28]. Here the GA-based penalty function method is also employed for solving the problem.

With above definition of the bonds on the design variables, the optimization problem leads to a large design domain. Thus, direct application of GAs may not yield good results. In order to obtain a solution closest to global optimum, the design space have to be further constrained. Therefore, four different approaches are used to restrict the number of design variables.

1. *Approach* 1: Each PCLD patch consists of the four design variables defined earlier, namely, the axial location, angular location, axial length and angular length.
2. *Approach* 2: Each PCLD patch consists of two design variables, namely the axial location and the angular location. The axial length and angular length are fixed and all patches are of same size. For a fixed mass of PCLD materials, different number of patches are obtained by fixing the axial length and varying the angular length of each PCLD patch. Therefore, as number of patches increases, the angular length of each patch decreases.
3. *Approach* 3: This is similar to Approach 2 except for the additional bounds imposed on the location for each patch. The surface of the cylinder are divided into two segments such that the number of patches are evenly distributed in each segments.
4. *Approach* 4: This is similar to Approach 3 except that the cylinder is divided into three ring segments instead of two ring segments in Approach 3.

4. Results and discussion

The geometric and material properties of the cylinder for implementing the PCLD treatment are shown in Table 1. The length and radius of the cylinder are, respectively, 0.35 and 0.1 m. The loss factor of viscoelastic material, η_v, and also its shear modulus, G_v, are assumed invariant with frequency. For comparison purpose, a small structural damping is introduced in the form of a complex elastic modulus for the base shell and the constraining layers: $E = \tilde{E}(1 + j\eta)$, where η is the structural loss factor. A η value of 0.0001 is used. With this setup, GA is applied to the optimization problem for each of the approaches outlined. For each set of parameters, defined in terms of the total amount of PCLD material, the number of patches and the approach used, five runs are executed to arrive at the layout with the lowest SVD of the cylinder.

Table 1
Properties of materials used in analysis of cylindrical shell

Properties	Shell (aluminum)	Constraining material	Viscoelastic material
Elastic modulus, $\tilde{E}$ (GPa)	$70(1+0.0001j)$	$49(1+0.0001j)$	—
Density, ρ (kg/m^3)	2.71×10^3	7.50×10^3	1.00×10^3
Thickness, h (m)	0.002	0.0002	0.0002
Shear modulus, G (MPa)	—	—	$0.896(1+0.5j)$

Table 2
Cylinder resonant frequencies below maximum excitation frequency

Mode (m,n)	Natural frequency (Hz)
(1,3)	818
(1,4)	906
(1,5)	1285
(1,2)	1376
(2,4)	1643
(2,5)	1648
(2,3)	2212

A unit harmonic transverse force is applied at the middle cylinder, i.e., $\theta^* = 0$ and $x^* = L/3$, and the excitation frequency is from $f = 0$ Hz to 3.2 kHz where $f = \omega/2\pi$. Before performing the optimization, the analytical model and associated solution procedure are validated by comparing the natural frequencies of bare cylinder with the theoretical predictions given in Ref. [25]. For cylinder with PCLD treatment, the frequency response at the force location is compared to results obtained by a multi-physics finite element code. The cylinder with single PCLD patch treatment is considered. Good agreements between the values are observed for both cases.

For the convenience of the discussion that follows, resonant frequencies of the seven modes of the considered cylinder within the excitation frequency range are listed in Table 2.

4.1. Comparison of four optimization approaches

For each of the four optimization approaches, the optimal layouts for different number of patches for a fixed total amount of PCLD material equivalent to an added weight of 2.4% are obtained. The reduction in SVD achieved, R_{SVD}, based on these layouts are shown in Fig. 3 where the dB values in Y-axis is calculated by

$$R_{SVD}(\omega) = 20\log\left(\frac{D(\omega)}{D_0(\omega)}\right)(\text{dB}), \tag{20}$$

where $D_0(\omega)$ and $D(\omega)$ are SVDs of the cylinder at circular frequency, ω, without and with PCLD patches.

The figure indicates that a good optimal layout cannot be easily obtained based on Approach 1, as indicated by the lower reduction achieved and irregularity in the reduction achieved. This may

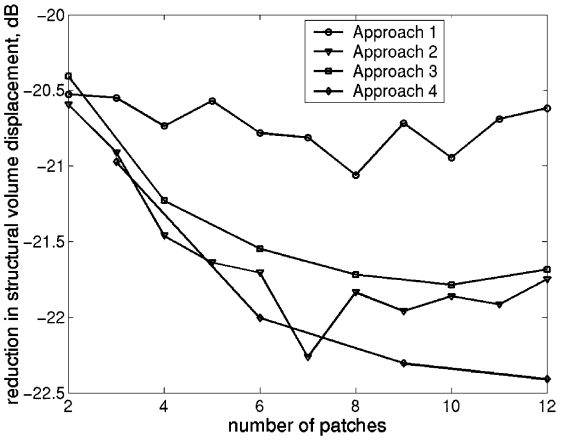

Fig. 3. Comparison of optimal solutions obtained based on the four approaches outlined.

due to the large resulting design space and under such environment, there is higher likelihood that the result obtained from GA is dominated by a few moderately good design which prevent further innovation.

On the other hand, Approach 4 (dividing the cylinder surface into 3 ring segments) is the best approach since the optimal layouts obtained consistently give the largest reduction in SVD. With Approach 2, although it gives an optimal layout also with large reduction in SVD using the least number of patches, regularity in the reduction achieved cannot be achieved. As for Approach 3 (dividing the cylinder surface into three ring segments), the reduction achieved is consistently lower than Approaches 2 and 4. This result indicates that a well-behaved problem must be suitably constrained to reduce the possible design space, but the constraints imposed must not preclude the actual optimal solution.

4.2. Attributes of number of PCLD patches

Further examining the results shown in Fig. 3, it is indicated that Approaches 2–4 show similar trends in the results in which the SVD decreases with diminishing reduction when the number of patches increases. Beyond a certain number of patches, further reduction achieved becomes negligible. The fact that the trend is not dependent on the approach used implies that this is an intrinsic property of the system. In particular, reviewing the optimal solutions obtained using Approach 4, it can be seen that when the number of patches is increased from 3 to 6, about 1 dB reduction in the cylinder SVD could be achieved. However, when the number of patches is further doubled, the SVD reduction obtained is only 0.4 dB. So for the considered cylinder and the excitation condition here, under the constraint of 2.4% PCLD added mass, it is deduced that the optimal number of patches is between 6 and 8.

The layouts obtained using Approach 4 for the cases of 3-, 6-, 9- and 12-patch are shown in Fig. 4. Non-dimensional axial and circumferential co-ordinates of the central locations, $(\theta_0/2\pi, z_0/L)$, of all optimal patches shown in the figure are given in Table 3.

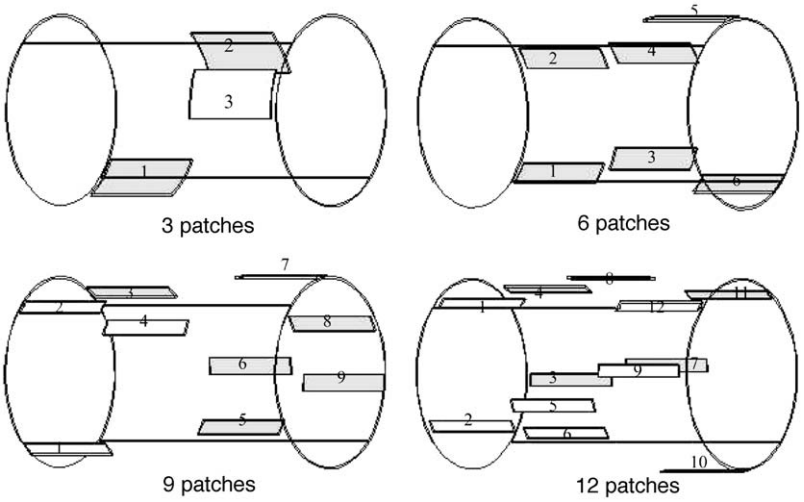

Fig. 4. PCLD patches layout obtained using Approach 4.

Table 3
Non-dimensional axial (x_0/L) and circumferential ($\theta_0/2\pi$) co-ordinates of central locations of the patches shown in Fig. 4

No. of patches	Co-ordinates	S/N of patch											
		1	2	3	4	5	6	7	8	9	10	11	12
3	Axial	0.184	0.515	0.831									
	Circum.	0.500	0.789	0.125									
6	Axial	0.177	0.177	0.529	0.574	0.809	0.860						
	Circum.	0.528	0.814	0.569	0.819	0.950	0.500						
9	Axial	0.162	0.162	0.162	0.493	0.507	0.500	0.824	0.838	0.853			
	Circum.	0.486	0.004	0.867	0.047	0.531	0.689	0.931	0.811	0.642			
12	Axial	0.177	0.184	0.184	0.191	0.500	0.515	0.522	0.515	0.824	0.830	0.846	0.853
	Circum.	0.004	0.289	0.661	0.867	0.247	0.319	0.722	0.931	0.147	0.000	0.864	0.375

4.3. Attributes of an optimal layout

Optimal layouts with different number of patches obtained using Approaches 2–4 are examined to determine the attributes of an optimal layout. As shown in Fig. 5 for the case of 12-patch used, the layout obtained using Approach 4 that gives the largest reduction, the patches tend to increase coverage in the axial direction rather than the angular direction. On the other hand, in Approach 3 in which the patches cannot maximize its coverage in axial direction due to the constraints imposed, lower reduction in SVD is observed. In addition, Approach 2, in which the

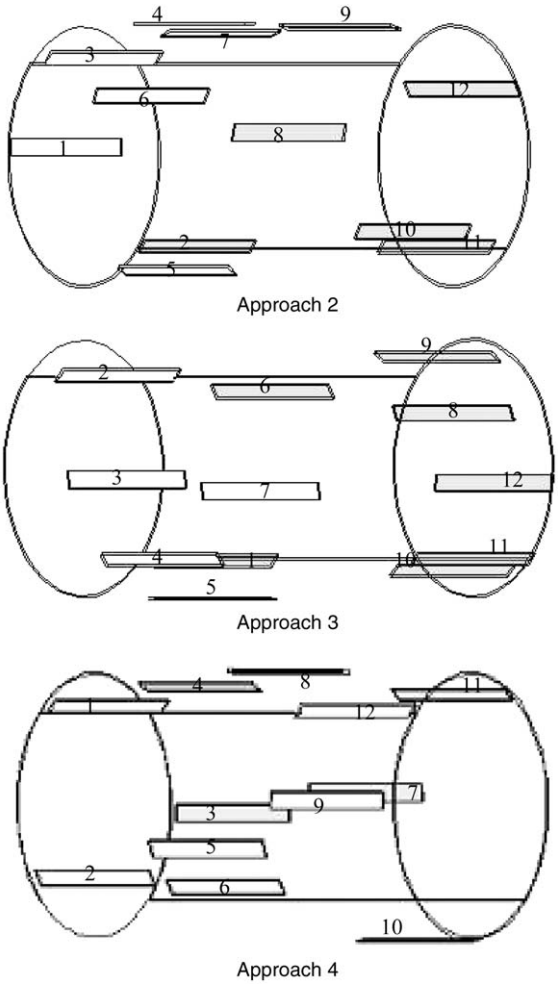

Fig. 5. Comparison of optimal layout for configuration using 12 patches.

Table 4
Non-dimensional axial (x_0/L) and circumferential ($\theta_0/2\pi$) co-ordinates of central locations of the patches shown in Fig. 5

Approach	Co-ordinates	S/N of patch											
		1	2	3	4	5	6	7	8	9	10	11	12
2	Axial	0.157	0.157	0.193	0.314	0.343	0.364	0.429	0.357	0.700	0.726	0.814	0.857
	Circum.	0.506	0.139	0.986	0.917	0.375	0.044	0.944	0.722	0.903	0.561	0.506	0.792
3	Axial	0.189	0.230	0.311	0.344	0.345	0.318	0.655	0.770	0.811	0.811	0.872	0.858
	Circum.	0.500	0.000	0.172	0.500	0.417	0.800	0.208	0.767	0.861	0.486	0.500	0.617
4	Axial	0.177	0.184	0.184	0.191	0.500	0.515	0.522	0.515	0.824	0.830	0.846	0.853
	Circum.	0.004	0.289	0.661	0.867	0.247	0.319	0.722	0.931	0.147	0.000	0.864	0.375

patches' positions are not constrained, also arrived at similar layout obtained using Approach 4. This indicates that maximization of coverage in the axial direction is an attribute of an optimal layout since it is independent of the approach used. Furthermore, in all three layouts shown in Fig. 5, the patches tend to distribute over the whole surface of the cylinder. This is thus another attribute of an optimal layout.

Table 4 gives the non-dimensional axial and circumferential co-ordinates of the central locations, $(\theta_0/2\pi, z_0/L)$, of all optimal patches shown in Fig. 5.

Based on the above observations, a general layout shown in Fig. 6 is proposed for a configuration with 12 patches. It resembles the spatially distributed cosine shaped sensor layout

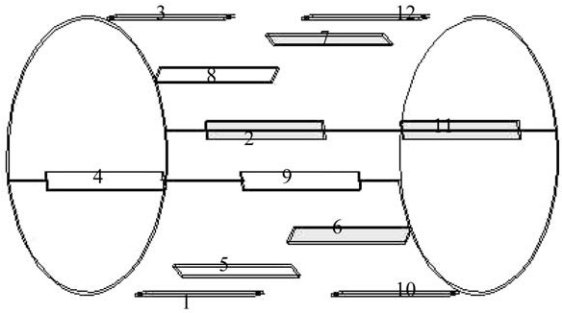

Fig. 6. PCLD patches layout approximated by the spatially distributed cosine shaped layout.

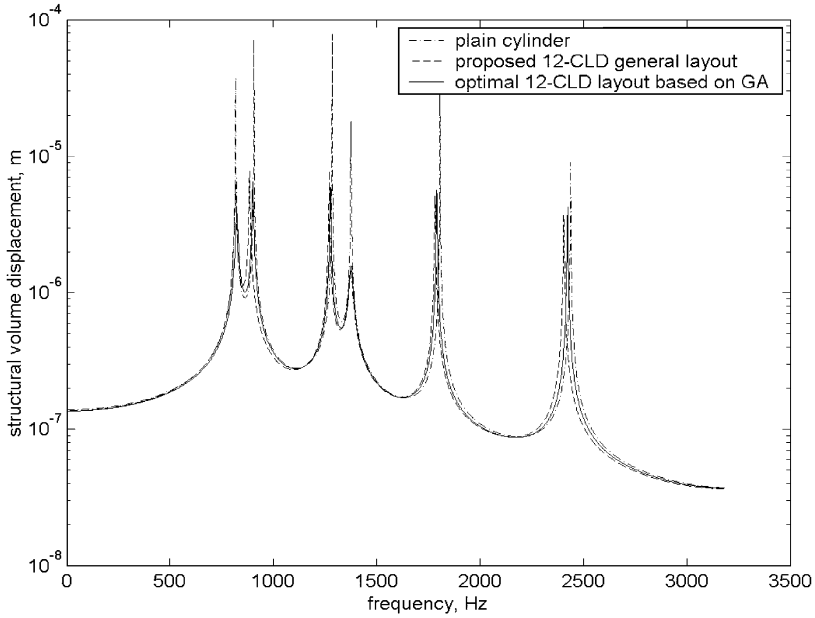

Fig. 7. SVDs of the cylinder with PCLD layouts obtained using (i) the spatially distributed cosine shaped layout and (ii) that by Approach 4.

developed in Ref. [29] for ASAC. The reduction of SVD obtained based on this general layout is 20.0 dB. This reduction is 2.4 dB less than the reduction resulting from the best layout obtained based on Approach 4. The SVDs of the cylinder with these two PCLD layouts and comparison with that of the plain cylinder are shown in Fig. 7. More displacement reduction are observed at resonant frequencies of lower mode order than higher more order, e.g., the largest SVD reduction is achieved at (1,2)th mode frequency, followed by significant reduction at (1,3)th mode frequency. The SVD reductions at other five mode frequencies are different from each other but, through PCLD layout optimization, the global displacement responses of the cylinder at these resonant frequencies are nearly in same level, although they are so different in magnitude for the bare cylinder.

4.4. *Effects of the patches' aspect ratio*

To determine the influence of the patches' shape on the SVD reduction achieved and since only rectangular patches are used, a dimensionless parameter, aspect ratio, i.e., the ratio of axial length to angular length of the patch, is defined to characterize the shape. The results, as shown in Fig. 8 for the case with 12-patch, indicate that the reduction of the SVD decreases when the ratio is decreased. This is consistent with the previous observation where we found that in an optimal layout, the patches tend to increase coverage in the axial direction rather than the angular direction. Thus, patches with large ratio of axial length to the angular length should be used in the layout design. Numerical results for the other considered case show similar trends.

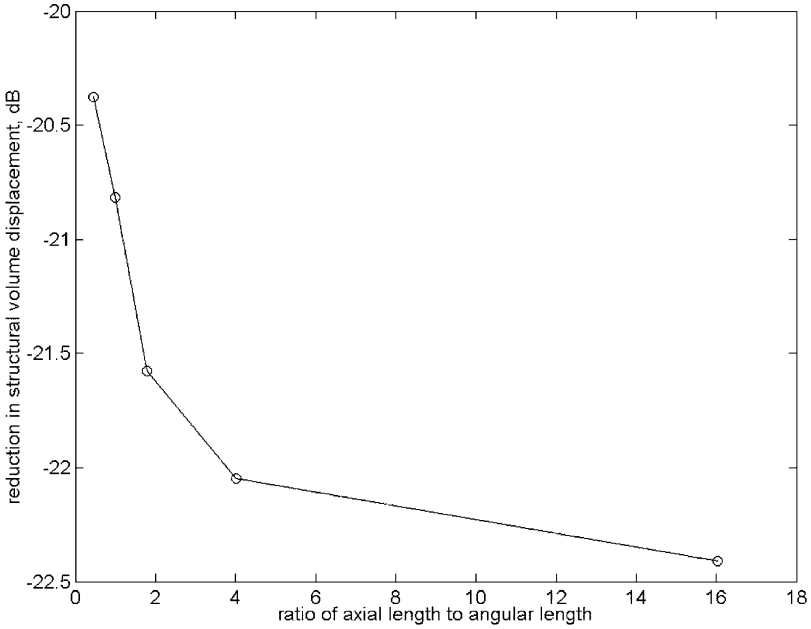

Fig. 8. Variation of SVD with aspect ratio of the patches.

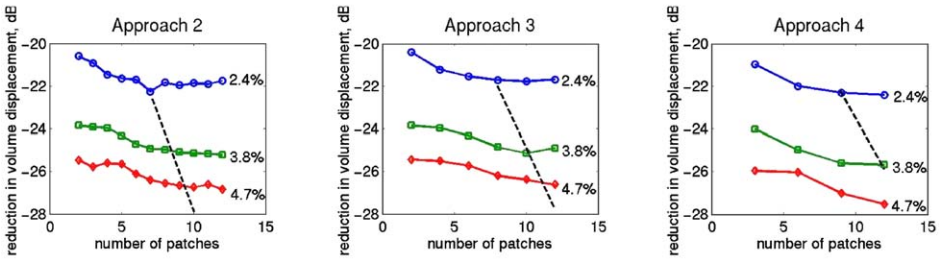

Fig. 9. Effects of increasing the total amount of PCLD patches used.

4.5. *Effects of total amount of PCLD used*

The result is shown in Fig. 9 where the percentage shown is the percentage of added weight of PCLD patches to the weight of base cylinder. It can be seen that the degree of vibration attenuation achieved increases as the total amount of PCLD materials increases. The optimal numbers of patches are indicated by the dashed line in the figure. These results imply that greater structural volume displacement reduction can be achieved when the PCLD patches are spread out over the whole surface of the cylinder.

5. Conclusion

The optimization of the layout of PCLD patches for (SVD) reduction of a simply supported cylinder excited by a broadband transverse force is presented in this paper. An analytical model is developed using the energy method to relate the SVD of cylinder to the physical parameters of the base cylindrical shell and all PCLD patches for the treatment. GA-based penalty function method is employed to optimize PCLD patches' locations and dimensions with the aim of minimizing the structural displacement response under given constraint of total amount of PCLD used. The optimal analyses indicate that for a fixed number of patches and amount of PCLD material, there are two attributes of an optimal layout. First, the patches tend to increase their coverage in the axial direction; and second, the patches tend to distribute over the whole surface of the cylinder. Other optimal analysis findings include that rectangular patches with large ratio of axial length to angular length produce better damping effects; and the degree of vibration attenuation of the cylinder with PCLD treatment increases with the increase of the total amount of PCLD materials used.

It is worth to point out that the work presented in this paper is limited to the case where the cylinder is simply supported at its two ends. It is, therefore, meaningful to carry out further study to examine the influence of boundary conditions on optimum of PCLD layout for minimizing its vibration response. Furthermore, volume displacement of the cylindrical shell is considered as the cost function to be minimized. So one more meaningful work is to perform the optimization study of PCLD layouts targeting to minimize other objective functions indicating the vibration response of the cylinder and associated sound radiation such as mean-square velocity, farfield pressure at pre-determined field points, and radiated sound power from whole vibrating structure.

References

[1] E.M. Kerwin Jr., Damping of flexural waves by a constrained viscoelastic layer, *Journal of the Acoustical Society of America* 31 (1959) 952–962.

[2] R.A. DiTaranto, Theory of vibratory bending for elastic and viscoelastic layered finite-length beams, *American Society of Mechanical Engineers Journal of Applied Mechanics* 32 (1965) 881–886.

[3] D.J. Mead, S. Markus, The forced vibration of a three-layer, damped sandwich beam with arbitrary boundary conditions, *Journal of Sound and Vibration* 10 (1969) 163–175.

[4] D.K. Rao, Frequency and loss factors of sandwich beams under various boundary conditions, *International Journal of Mechanical Engineering Science* 20 (1978) 271–278.

[5] M.J. Yan, E.H. Dowell, Governing equations of vibrating constrained-layer damping sandwich plates and beams, *American Society of Mechanical Engineers Journal of Applied Mechanics* 94 (1972) 1041–1047.

[6] M.D. Rao, S. He, Dynamic analysis and design of laminated composite beams with multiple damping layers, *American Institute of Aeronautics and Astronautics Journal* 31 (1993) 736–745.

[7] K.S. Rao, B.C. Nakra, Theory of vibratory bending of unsymmetrical sandwich plates, *Archives of Mechanics* 25 (1973) 213–225.

[8] K.M. Ahmed, Dynamic analysis of sandwich beams, *Journal of Sound and Vibration* 21 (1972) 263–276.

[9] C.D. Johnson, D.A. Kienholz, Finite element prediction of damping in structures with constrained viscoelastic layers, *American Institute of Aeronautics and Astronautics Journal* 20 (1982) 1284–1290.

[10] D.S. Nokes, F.C. Nelson, Constrained layer damping with partial coverage, *Shock and Vibration Bulletin* 38 (1968) 5–10.

[11] A.K. Lall, N.T. Asnani, B.C. Nakra, Damping analysis of partially covered sandwich beams, *Journal of Sound and Vibration* 123 (1988) 247–259.

[12] A.K. Lall, N.T. Asnani, B.C. Nakra, Vibration and damping analysis of rectangular plate with partially covered constrained viscoelastic layer, *American Society of Mechanical Engineers Journal of Vibration, Acoustics, Stress, and Reliability in Design* 109 (1987) 241–247.

[13] S.W. Kung, R. Singh, Vibration analysis of beams with multiple constrained layer damping patches, *Journal of Sound and Vibration* 212 (5) (1998) 781–805.

[14] H.H. Pan, Axisymmetrical vibrations of a circular sandwich shell with a viscoelastic core layer, *Journal of Sound and Vibration* 9 (1969) 338–348.

[15] I.W. Jones, V.L. Salerno, Analysis of free damped vibration of laminated composite plates and shells, *International Journal of Solids and Structures* 25 (1990) 129–149.

[16] N. Alam, N.T. Asnani, Vibration damping analysis of a multilayered cylindrical shell, Part I: theoretical analysis, *American Institute of Aeronautics and Astronautics Journal* 22 (1984) 803–810.

[17] N. Alam, N.T. Asnani, Vibration damping analysis of a multilayered cylindrical shell, Part II: numerical results, *American Institute of Aeronautics and Astronautics Journal* 22 (1984) 975–981.

[18] T.C. Ramesh, N. Ganesan, Vibration and damping analysis of cylindrical shells with constrained damping treatment—a comparison of three theories, *American Society of Mechanical Engineers Journal of Vibration and Acoustics* 117 (1995) 213–219.

[19] Y.C. Hu, S.C. Huang, The frequency response and damping effect of three-layer thin shell with viscoelastic core, *Computers and Structures* 76 (2000) 577–591.

[20] L.H. Chen, S.C. Huang, Vibrations of a cylindrical shell with partially constrained layer damping (CLD) treatment, *International Journal of Mechanical Science* 41 (1999) 1485–1498.

[21] L.H. Chen, S.C. Huang, Vibration attenuation of a cylindrical shell with partially constrained layer damping strips treatment, *Computers and Structures* 79 (2001) 1355–1362.

[22] J.L. Marcelin, P. Trompette, A. Smati, Optimal constrained layer damping with partial coverage, *Finite Elements in Analysis and Design* 12 (1992) 273–280.

[23] J.L. Marcelin, S. Shakhesi, F. Pourroy, Optimal constrained layer damping of beams: experimental numerical studies, *Shock and Vibration* 2 (1995) 445–450.

[24] Y.C. Chen, S.C. Huang, An optimal placement of CLD treatment for vibration suppression of plates, *International Journal of Mechanical Science* 44 (2002) 1801–1821.

[25] W. Soedel, *Vibrations of Plates and Shells*, 2nd Edition, Marcel Dekker, New York, 1993.
[26] A. Berry, Advanced sensing strategies for the active control of vibration and structural radiation, *Noise Control Engineering Journal* 49 (2001) 54–65.
[27] S.S. Rao, *Engineering Optimization—Theory and Practice*, 3rd Edition, Wiley, New York, 1996.
[28] A. Osyczka, *Evolutionary Algorithms for Single and Multicriteria Design Optimization*, Physica-Verlag, Heidelberg, 2002.
[29] H.S. Zhou, J.P. Zhong, M. Natori, Sensor mechanics of distributed shell convolving sensors applied to flexible rings, *American Society of Mechanical Engineers Journal of Vibration and Acoustics* 115 (1993) 40–46.